

The X-ray Lightcurve of η Carinae: Refinement of the Orbit and Evidence for Phase Dependent Mass Loss

M. F. Corcoran^{1,2}, K. Ishibashi³, J. H. Swank², R. Petre²

ABSTRACT

We solve the *RXTE* X-ray lightcurve of the extremely luminous and massive star η Carinae with a colliding wind emission model to refine the ground-based orbital elements. The sharp decline to X-ray minimum at the end of 1997 fixes the date of the last periastron passage at 1997.95 ± 0.05 , not 1998.13 as derived from ground-based radial velocities. This helps resolve a discrepancy between the ground-based radial velocities and spatially-resolved velocity measures obtained by STIS. The X-ray data are consistent with a mass function $f(M) \approx 1.5$, lower than the value $f(M) \approx 7.5$ previously reported, so that the masses of η Carinae and the companion are $M_\eta \geq 80M_\odot$ and $M_c \sim 30M_\odot$, respectively. In addition the X-ray data suggest that the mass loss rate from η Carinae is generally less than $3 \times 10^{-4} M_\odot \text{ yr}^{-1}$, about a factor of 5 lower than that derived from some observations in other wavebands. We could not match the duration of the X-ray minimum with any standard colliding wind model in which the wind is spherically symmetric and the mass loss rate is constant. However we show that we can match the variations around X-ray minimum if we include an increase of a factor of ~ 20 in the mass loss rate from η Carinae for approximately 80 days following periastron. If real, this excess in \dot{M} would be the first evidence of enhanced mass flow off the primary when the two stars are close (presumably driven by tidal interactions). Our interpretation of the X-ray data suggest that the *ASCA* and *RXTE* X-ray spectra near the X-ray minimum are significantly contaminated by unresolved hard emission ($E \geq 2 \text{ keV}$) from some other nearby source, probably associated with scattering of the colliding wind emission by circumstellar dust. Based on the X-ray fluxes the distance to η Carinae is 2300 pc with formal uncertainties of only $\sim 10\%$.

Subject headings: η Carinae, stars: X-rays, stars: binaries

¹Universities Space Research Association, 7501 Forbes Blvd, Ste 206, Seabrook, MD 20706

²Laboratory for High Energy Astrophysics, Goddard Space Flight Center, Greenbelt MD 20771

³National Research Council, Laboratory For Astronomy and Space Physics, Goddard Space Flight Center, Greenbelt, MD 20771

1. Introduction

Discovery of cyclical variations in the strength of the He I 10830Å line (Damineli 1996), the X-ray flux (Corcoran et al. 1995; Ishibashi et al. 1999) and radio emission (Duncan et al. 1995) spurred the suggestion that the supermassive star η Carinae is in fact a binary system (Damineli 1996; Damineli, Conti and Lopes 1997; Corcoran et al. 1997) in which the variable phenomena over all wavelengths is driven by wind-wind interactions. Since the formation and evolution of massive binaries proceeds via mechanisms distinct from those available to single stars (Vanbeveren, De Loore, and Van Rensbergen 1998), the presence of a companion would have a profound impact on our understanding of the formation and evolution of η Carinae in particular and of extremely massive stars in general, and it is essential that we resolve this issue one way or another.

However, the “binary model” as proposed faces three major observational difficulties. The first concerns the variation of the X-ray emission from the source as measured by the Rossi X-ray Timing Explorer (*RXTE*, Bradt et al. 1993). First attempts to model the observed *RXTE* 2–10 keV X-ray variability (Ishibashi et al. 1999) showed qualitative similarities to the observed variations in flux and column density but could not describe the X-ray variability near the X-ray minimum if the orbital elements derived from ground-based radial velocity data (Damineli, Conti and Lopes 1997; Davidson 1997) were assumed. A second problem is that the column density to the X-ray source as measured by the *ASCA* satellite (Tanaka, Inoue, and Holt 1994) is lower, not higher, than the value outside eclipse and no increase in flux was seen to energies of 10 keV, in contrast to model predictions (Corcoran et al. 2000). Finally, expected radial velocity variations (Damineli, Lopes and Conti 1999) were not confirmed by subsequent HST/STIS observations of the stellar emission resolved from contamination by nearby circumstellar emission (Davidson et al. 2000). A more recent solution of the ground-based data (Damineli et al. 2000) does better to reconcile the velocity curve with the STIS measurements but does not adequately resolve the problems with the observed X-ray variations. Since the only observable spectral features are emission lines, there is the real possibility that the variation of the emitting gas may not faithfully represent the motion of the star, which means that deriving a true stellar radial velocity curve from the emission line analysis alone may be difficult no matter what spatial resolution is available.

A more recent analysis of the *RXTE* data by Ishibashi (1999) showed that the match between the model and the X-ray lightcurve could be improved if the orbital elements were relaxed from the ground-based values. Here we try to use the X-ray lightcurve to attempt to refine the orbit. We find that we can generate an improved match to the *RXTE* fluxes if the time of periastron passage is earlier, the eccentricity higher and the mass function lower than given in the Damineli et al. (2000) orbital solution. Most importantly, we find that the width of the X-ray minimum requires a suppression of the observed flux for an extended period following periastron. One way to do this is by a temporary large increase (by a factor of 20) in the mass loss rate from η Carinae for a brief period just after periastron passage. In the rest of the paper we describe our analysis of the X-ray lightcurve. In §2 we discuss the data extraction. In §3 we describe the colliding wind model and discuss our attempts to solve the X-ray lightcurve, and in §4 we present our conclusions.

2. Observations and Data Reduction

We use data obtained by the *RXTE* Proportional Counter Array (PCA). Data extraction, and instrumental background correction, are as described in Ishibashi et al. (1999). Most of the early data were obtained using 3 proportional counter units (PCUs), though we also include scaled 2-PCU mode data in the lightcurve, since most of the data available after 1998 is in 2-PCU mode. To convert these rates to flux, we use a linear conversion derived by comparison of *RXTE* and spatially resolved X-ray fluxes measured by contemporaneous observations of η Carinae with the *ASCA* X-ray satellite. There are four *ASCA* observations which overlap *RXTE* pointings within 2 days or less. We derived source fluxes from the *ASCA* data by direct fitting of the extracted spectrum corrected for instrumental background and for sky background (where “sky” is the region beyond the 3' radius circle used to extract the *ASCA* source spectrum). We then compared these fluxes to the *RXTE* count rate corrected for instrumental background. Figure 1 shows the *ASCA* fluxes and the *RXTE* net rates. A fit to these data yields $flux = 0.26(N - 7.66)$, where $flux$ is the 2–10 keV flux seen by *RXTE* (in units of 10^{-11} ergs cm^{-2} s^{-1}), and N is the *RXTE* 3-PCU rate corrected for instrumental background. Thus the sky background contributes about 7.66 counts s^{-1} to every 3-PCU observation. This value is slightly lower than the value used in Ishibashi et al. (1999) by about 1 count s^{-1} per 3 PCUs.

We also included *RXTE* “quicklook” data for the period since mid 1998. For each observation, we extracted PCA rates for the intervals when the satellite was on target; we then corrected these data for instrumental background in the same manner as used for the processed data. Since many of these data were obtained in 2 PCU mode we performed an additional scaling to correct the 2 PCU data to approximate 3 PCU rates. We compared these net rates to the *RXTE* fluxes derived from the processed data in the intervals of overlap. We found that the scaling from the corrected quicklook net rates to observed 2–10 keV flux is $flux = 0.29(N_{ql} - 8.86)$, where $flux$ is the 2–10 keV flux (in units of 10^{-11} ergs cm^{-2} s^{-1}) and N_{ql} the corrected quicklook rates.

Figure 2 shows the *RXTE* lightcurve in the interval February 1996 through March 2000. This lightcurve includes the data published in Ishibashi et al. (1999) and more recent observations. For our purposes, the significant characteristics are these: 1) a gradual increase in count rate starting at 1997.0; 2) a rapid rise to maximum and even faster decline to minimum at the end of 1997; 3) a gradual brightening of the X-ray flux coming out of the X-ray minimum; and 4) asymmetric maxima just prior to and just after the X-ray eclipse. Also apparent in the lightcurve are higher frequency “flares” (Corcoran et al. 1997; Ishibashi et al. 1999); in what follows we make no attempt to try to explain or fit these higher-frequency variations.

3. X-ray Lightcurve Analysis

The colliding wind emission model we use is based on the Usov (1992) model used in Ishibashi et al. (1999). We fix the period of the binary orbit at 5.52 years (Damineli 1996), since this value

seems to describe the He I 10830Å variations (Damineli 1996), the radio variability (Duncan et al. 1995) and the recurrent X-ray low state (Ishibashi et al. 1999). We take the the orbital elements as given in Damineli et al. (2000) as a starting point, and, since the variations in He I 10830Å and the radio emission suggest an eclipse of a source of UV radiation presumably provided by the companion (Damineli, Conti and Lopes 1997; Duncan et al. 1995), we consider solutions in which the companion is a strong source UV source, which restricts the mass of the companion to $M_c > 15M_\odot$. We further assume that the winds collide at terminal velocities, and take $V_{\infty,\eta} = 500$ km s⁻¹ (Hillier et al. 2000) and $V_{\infty,c} = 2000$ km s⁻¹ as reasonable values for the terminal velocities of η Carinae and the companion, respectively.

3.1. A Constant \dot{M} Model

Table 1 lists the parameters we used to derive the model curves presented in figure 2. After some experimenting, we adopted mass loss rates $\dot{M}_\eta = 1 \times 10^{-4} M_\odot \text{ yr}^{-1}$ for η Carinae, and $\dot{M}_c = 1 \times 10^{-5} M_\odot \text{ yr}^{-1}$ for the companion. We adopted $80M_\odot$ as the mass for η Carinae. We found that a companion mass of $M_c \sim 30M_\odot$ provided a suitable fit to both the X-ray lightcurve and the STIS radial velocities. These component masses are similar to those described by Davidson (1999). However, our analysis is not very sensitive to the values of the component masses, and we find that we can fit the X-ray and STIS data with larger values of η Carinae’s mass, or smaller component masses, or some combination. We allowed the eccentricity e , time of periastron passage T_o , and the terminal velocity of the wind of η Carinae $V_{\infty,\eta}$ to vary to improve the fit to the *RXTE* lightcurve. We found that in order to match the rapid drop in X-ray brightness, the value of ω needed to be near 270° with periastron passage $T_o = 1997.95$, with an estimated uncertainty in T_o of ± 0.05 years. These parameters ensure that the line of sight at periastron passes through the thickest part of the wind from η Carinae if $i < 60^\circ$. While our adopted value of ω is the same as that of Damineli et al. (2000), the sharp decline to minimum in the X-ray data fixes periastron passage to occur about 73 days earlier than the Damineli et al. (2000) value. We also derive an eccentricity $e = 0.9$, which is higher than the highest previously published value, $e = 0.8$ (Davidson 1999). The smooth solid curve in figure 2 is the colliding wind emission based on our adopted parameters; the model based on the Damineli et al. (2000) values given in table 1 is shown by the thick broken line. Our model is an improvement over those published previously (Pittard et al. 1998; Ishibashi et al. 1999) in that the decline to minimum and the asymmetry of the shoulders of the eclipse are better matched (though the model badly fails to match the observed eclipse duration). The ratio of the model flux to the observed X-ray flux determines the distance to η Carinae as $D \approx 2300$ pc. The formal uncertainty in the distance we derive is primarily influenced by uncertainties in fixing the X-ray flux level outside of the eclipse, and is only about 10%. However, uncertainties in the model parameters and other simplifications in the analytic description of the X-ray luminosity may make the real uncertainty in the distance somewhat larger.

The values of \dot{M} listed in table 1 are rather uncertain; in particular we have adopted a rather

large value for the mass loss rate of the companion, i.e. $\dot{M}_c = 10^{-5} M_\odot \text{ yr}^{-1}$, which would suggest that the companion is an evolved WR-type star. While the adopted values provide a fairly good match to most of the observed X-ray variability (outside of X-ray minimum), these mass-loss rates are not uniquely defined. Other combinations of \dot{M}_η and \dot{M}_c can also provide an adequate match to the data, especially if we allow some latitude in choice of terminal velocities. In order to see if any constraints could be placed on mass loss rates, we ran models with differing values of \dot{M} for both stars, with the wind terminal velocities and orbital elements held constant at the tabulated values. We found that the mass loss rate from η Carinae is constrained to be $\dot{M}_\eta < 3 \times 10^{-4} M_\odot \text{ yr}^{-1}$ in order to match the gradual rise to maximum in the 1997.0–1997.9 interval. Models with \dot{M}_η larger than this limit show significant absorption of the 2–10 keV X-ray emission months prior to periastron, which suppresses the rise in L_x up to periastron. In addition these models generally yield columns of $N_H > 10^{23} \text{ cm}^{-2}$ at all orbital phases, while the observed columns are typically $N_H \approx 3 \times 10^{22} \text{ cm}^{-2}$ for most of the orbit (?). As an example of this effect, we include in figure 2 a model with $\dot{M}_\eta = 3 \times 10^{-4} M_\odot \text{ yr}^{-1}$. This model is basically flat through 1997 except for a very brief increase in observed flux very near periastron, in contrast to the observed X-ray variation during this interval. It is more difficult to put constraints on the mass loss rate from the companion, since the X-ray lightcurve in the 1996–2000 interval is dominated by the wind from η Carinae. Observations near inferior conjunction/apastron (in 2002.25) may allow us to put tighter constraints on \dot{M}_c as the companion moves in front of η Carinae.

3.2. An Enhanced \dot{M} Model

While the new orbit model provides an adequate match to the decline to minimum, the width of the eclipse in the model is still much narrower than the observed X-ray eclipse. This is mainly due to the fact that, for any significant orbital eccentricity, the stars move very quickly near periastron so that the line of sight quickly passes through less dense regions of the wind from η Carinae as the orientation to the colliding wind shock changes. As noted by Corcoran et al. (2000), however, the anomalously small column density measured by *ASCA* during the X-ray eclipse, and the lack of any enhancement in emission out to 10 keV at that time, may well indicate that the colliding wind source is completely hidden, and that the measured emission is simply contamination from another source of keV X-rays within the source extraction region (i.e. within $3'$ from η Carinae). Corcoran et al. (2000) noted that a column density $N_H > 10^{24} \text{ cm}^{-2}$ would be necessary to completely hide the colliding wind source. A column so large might imply either a non-spherical wind or disk around η Carinae (Ishibashi et al. 1999), or a mass loss increase near periastron if the wind from η Carinae is spherically symmetric away from the wind-wind collision shock. We attempted to model the X-ray lightcurve by allowing for a brief period of enhanced mass loss from η Carinae after periastron. Our best fit is shown as the solid smooth curve in figure 3. In this model we assume an increase of a factor of 20 in \dot{M}_η in the interval $T_o < t < T_o + 0.221$ years, i.e. we assume an interval of mass loss enhancement by a factor 20 starting at periastron passage and lasting for about 80 days. The model shown in figure 3 provides a much better match to the observed duration of the

X-ray eclipse. For comparison we also calculate a similar “enhanced- \dot{M}_η ” model with the orbital elements of Daminieli et al. (2000). This model is shown as the broken curve in figure 3. Figure 4 shows the variation in the model N_H relative to the constant \dot{M}_η model.

3.3. Expected and Observed Radial Velocities

From their STIS data, Davidson et al. (2000) determined velocity shifts in the range $-23 \leq \Delta v_{0.7} \leq -4 \text{ km s}^{-1}$ for the Pa 3-7, 3-8, 3-10, and 3-11 emission lines, where $v_{0.7}$ are the velocities they measured at 70% of the peak of the emission line. The velocities $v_{0.5}$ at 50% of the emission line peak lie in the range $-3 \leq \Delta v_{0.5} \leq +4 \text{ km s}^{-1}$. The emission line velocity shifts are much less than the expected shift $\Delta v \equiv (v(1999.1) - v(1998.2)) = +35 \text{ km s}^{-1}$ based on the orbital solution of Daminieli, Conti and Lopes (1997) and Daminieli, Lopes and Conti (1999), which Davidson et al. (2000) used for comparison to their STIS data. The orbital solution in Daminieli et al. (2000) implies that $v(1998.2) = +26 \text{ km s}^{-1}$ and $v(1999.1) = +24 \text{ km s}^{-1}$ or $\Delta v = -2 \text{ km s}^{-1}$, in better agreement with some of the STIS observations, though this solution still has serious problems in matching the observed X-ray lightcurve, as shown in figures 2 and 3. Figure 5 shows the Daminieli et al. (2000) radial velocity curve, and the radial velocity curve based on the “X-ray orbital elements” in Table 1. The vertical lines show the range of $v_{0.7}$ from Davidson et al. (2000) for their Paschen line measurements. The $v_{0.5}$ velocities show an even larger scatter than the $v_{0.7}$ velocities. Both the Daminieli et al. (2000) radial velocity curve and the curve based on the X-ray analysis show reasonable agreement with the STIS velocities.

4. Conclusions

Our attempts to model the *RXTE* lightcurve of η Carinae strongly suggest that:

1. η Carinae is a binary star in which the observed properties of the 2–10 keV X-ray emission are primarily due to wind-wind collisions;
2. if the luminosity of the X-ray source varies as the inverse of the separation of the stars, then the duration of the X-ray minimum is very difficult to fit in any colliding wind model with significant eccentricity and $i \leq 60^\circ$ unless the observed flux is artificially suppressed for an interval of time following periastron, possibly due to an enhancement in mass loss rate at that time.
3. the sharp decline to minimum requires that the periastron passage occurred at the end of 1997, and not in early 1998.

It could only be possible to keep the time of periastron passage as late as 1998.13 if there were a significant mass loss enhancement prior to periastron passage. Our preliminary exploration of

such models suggests that they do not match the observed decline from X-ray maximum to X-ray minimum as well as the model presented here. It is of course harder to conjecture physical reasons for an enhancement prior to periastron passage, though full illumination of this point requires detailed modeling of the tidal forces on η Carinae. The duration of the X-ray eclipse in the model could be extended without an enhancement in \dot{M}_η if the inclination is closer to 90° , since then the line of sight to the X-ray source passes through very dense regions of the wind from η Carinae for an extended period near conjunction. However large values of inclination seem ruled out by lack of optical variability. It is worth noting that, for values of i near 50° , and if the wind eclipse is complete, then conjunction must occur near periastron, since otherwise there is not enough wind material along the line of sight to produce much absorption at energies above 5 keV.

In a very eccentric orbit, the increase in tidal force near periastron provides an obvious explanation for an increase in \dot{M}_η at that time, especially if the outer layers of η Carinae are not tightly bound to the stellar core. The importance of tidally driven mass loss from η Carinae has been considered previously (for example, Davidson 1997). Even if $e = 0.9$, the periastron separation is still about $1.5 \text{ AU} = 320 R_\odot$, so the stars are not particularly close. However the radius of η Carinae is currently not well constrained, and probably lies in the range $70 - 450 R_\odot$ (Davidson 1999), so even in the conservative case the separation is only about 5 times the stellar radius of η Carinae. It is interesting to speculate that some of the line profile variability observed near periastron is actually produced by a combination of a change in radial velocity and a change in circumstellar density; if so, then radial velocity curves may be biased in some way near periastron passage.

Perhaps one of the more controversial results of our X-ray analysis is the rather low mass loss rate we derive for η Carinae. Typical values of \dot{M}_η are generally $\sim 10^{-3} M_\odot \text{ yr}^{-1}$, not $\sim 10^{-4} M_\odot \text{ yr}^{-1}$, which we claim as the true mass loss rate for η Carinae for most of the 5.52 year cycle. However, the mass loss rate from η Carinae is not well constrained by observations in other regions of the EM spectrum. Andriessse, Donn and Viotti (1978) derived a value of $\dot{M}_\eta \approx 7.5 \times 10^{-2} M_\odot \text{ yr}^{-1}$ based on their analysis of the dust formation rate, while van Genderen and The (1984) estimated that $\dot{M}_\eta \approx 10^{-4} M_\odot \text{ yr}^{-1}$ based on a number of arguments. Davidson (1987) gave $\dot{M}_\eta < 10^{-3} M_\odot \text{ yr}^{-1}$. Radio observations (White et al. 1994) yield $\dot{M}_\eta \approx 3 \times 10^{-4} M_\odot \text{ yr}^{-1}$. A STIS spectrum obtained in March 1998 (coincidentally near the time of our “enhanced mass loss” interval) and analyzed by Hillier et al. (2000) yielded a value of $\dot{M}_\eta \approx 10^{-3} M_\odot \text{ yr}^{-1}$. Millimeter observations (Cox et al. 1995; Cox 1997) yielded values of $\dot{M}_\eta \approx 10^{-3} M_\odot \text{ yr}^{-1}$. We should point out that most of these other mass loss rate estimates assume that η Carinae is a single star; this assumption neglects the effect of the companion on the ionization balance in the outer wind of η Carinae which in turn can significantly affect mass loss estimates which may be based on the strength of emission line profiles or the amount of free-free emission in the outer part of the wind. It is possible that by including the influence of the companion on the ionization of η Carinae’s wind, and/or the inclusion of wind variability, better agreement in the values of mass loss rate derived from analyses in different wavebands may be obtained.

While we have modelled the X-ray eclipse as an interval of enhanced X-ray absorption, an alternative possibility is that the long X-ray minimum might represent a reduction of the intrinsic X-ray emission. Such a reduction presumably could be produced if the winds near periastron collide at velocities much less than their terminal speeds. The relative collision velocities could be less near periastron if the winds from one or both stars have slower accelerations than winds from other massive stars, or if radiative braking (Gayley, Owocki, and Cranmer 1997) is important.

We expect that STIS (or other high spatial resolution) Paschen-line observations of the core of η Carinae near the next periastron passage (2003.5) will show large velocity shifts if the binary model presented here is correct, and the mass ratio is not too extreme. However, if significant variations in the ionization, the density and/or emitting volume near periastron passage occur, then determining accurate radial velocities and orbital elements from the emission lines may be difficult even with STIS. The X-ray fluxes however should be relatively insensitive to these effects. It may very well be that the variable P-Cygni absorption components seen in the STIS data (Hillier et al. 2000) may provide a good estimate of the stellar velocities, since the absorbing volume is constrained to lie in front of the stellar disk. Coordinated X-ray and STIS spectral observations of the P Cygni lines near periastron will be especially useful to fully constrain the orbit.

We thank Frank Chung, a student intern from the Eleanor Roosevelt High School, Greenbelt, MD, for his assistance in generating model fits to the *RXTE* lightcurve. We also thank Stan Owocki, Kris Davidson and the referee, David Cohen, for enlightening comments which have significantly improved this paper. This work made use of the FTOOLS suite of software supported by the HEASARC. The *RXTE* observations were supported by NASA grant NAS5-32490. This research has made use of NASA's Astrophysics Data System Abstract Service.

REFERENCES

- Andriessse, C. D., Donn, B. D. and Viotti, R. 1978, MNRAS, 185, 771
Bradt, H.V., Rothschild, R.E., and Swank, J.H. 1993, A&AS, 97, 355
Chlebowski, T., et al., 1984, ApJ, 281, 665
Corcoran, M. F., et al., 1995, ApJ, 445, L121
Corcoran, M. F., et al., 1997, Nature, 390, 587
Corcoran, M. F., et al., 1998, ApJ, 494, 381
Corcoran, M. F., et al., 2000, ApJ, in press
Cox, P., et al., 1995, A&A, 297, 168

- Cox, P., 1997, in ASP. Conf. Ser. 120, Luminous Blue Variables: Massive Stars in Transition, ed. A. Nota and H. J. G. L. M. Lamers (San Francisco: ASP), 277
- Damineli, A., 1996, ApJ, 460, L49
- Damineli, A., Conti, P. S., Lopes, D. F., 1997, New Astronomy, 2, 107
- Damineli, A., Lopes, D. F., and Conti, P. S., 1999, in ASP. Conf. Ser. 179, η Carinae at the Millennium,, ed. J. A. Morse, R. M. Humphreys, and A. Damineli (San Francisco: ASP), 288
- Damineli, A., Kaufer, A., Wolf, B., Stahl, O., Lopes, D. F., Araújo, F. X., 2000, ApJ, 528, L101
- Davidson, K. 1987, ApJ, 317, 760
- Davidson, K. 1997, New A, 2, 387
- Davidson, K., 1999, in ASP. Conf. Ser. 179, η Carinae at the Millennium,, ed. J. A. Morse, R. M. Humphreys, and A. Damineli (San Francisco: ASP), 6
- Davidson, K., Ishibashi, K., Gull, T. R., Humphreys, R. M., and Smith, N., 2000, ApJ, 530, L107
- Davidson, K., et al., 1986, ApJ, 305, 867
- Duncan, R.A., et al., 1995, ApJ, 441, L73
- Gayley, K., Owocki, S. P., and Cranmer, S., 1997, ApJ, 474, 786
- Hillier, D. J., Davidson, K., Ishibashi, K., and Gull, T., 2000, ApJ, submitted
- Ishibashi, K., et al., 1997, IAU Circ., 6668
- Ishibashi, K., et al., 1999, ApJ, 524, 983
- Ishibashi, K., 1999, Phd Thesis, University of Minnesota
- Pittard, J. M., Stevens, I. R., Corcoran, M. F., and Ishibashi, K., 1998, MNRAS, 299, L5
- Tanaka, Y., Inoue, H., Holt, S. S., 1994, PASJ, 46, L37
- Usov, V. V., 1992, ApJ, 389, 635
- Vanbeveren, V., De Loore, C., and Van Rensbergen, W., 1998, AARV, 9, 63
- van Genderen, A. M. and The, P. S. 1984, Space Science Reviews, 39, 317
- White, S. M., et al., 1994, ApJ, 429, 380

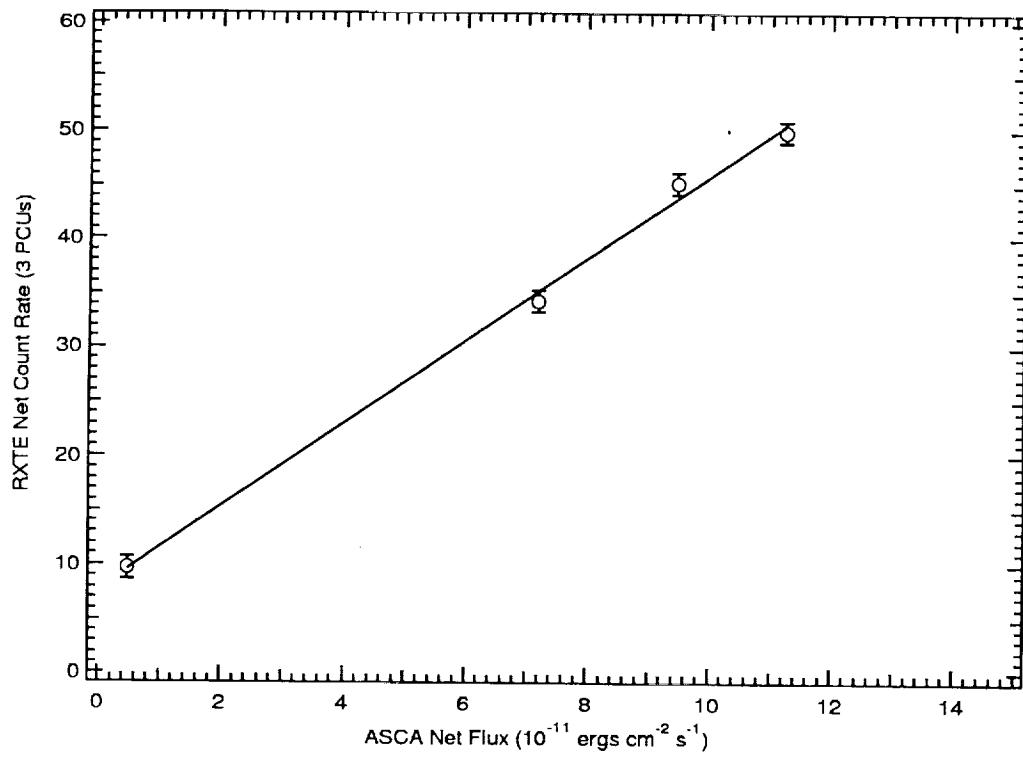
Fig. 1.— Plot of *RXTE* count rates versus contemporaneous *ASCA* 2–10 keV source flux. The *RXTE* rates have been corrected for instrumental background. The straight line shows the best fit to the data.

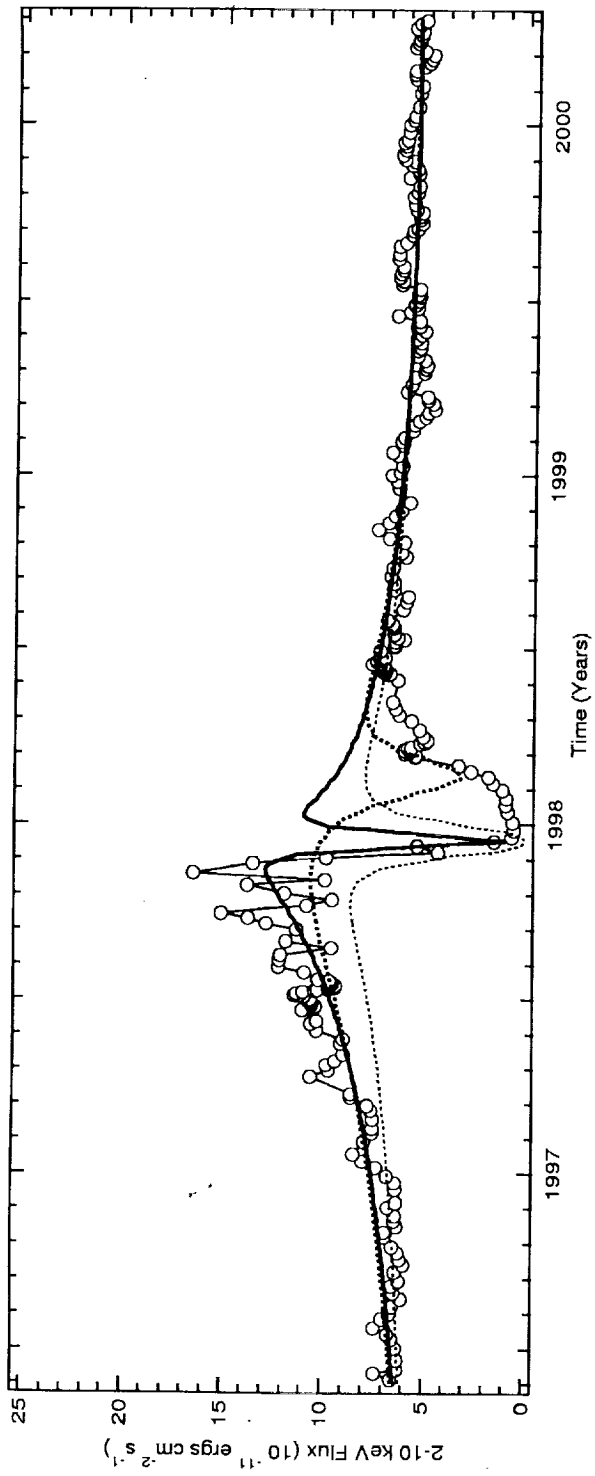
Fig. 2.— The *RXTE* lightcurve of η Carinae and the colliding wind model (thick solid line). The thick dotted line is the model derived using the orbital elements in Damineli et al. (2000), with $f(m) = 7.5$. The model based on the Damineli et al. (2000) parameters does not fit the abrupt decline in the observed 2–10 keV X-ray flux. Neither model fits the width of the X-ray eclipse adequately. The thin dotted line shows the effect of increasing \dot{M}_η to $3 \times 10^{-4} M_\odot \text{ yr}^{-1}$.

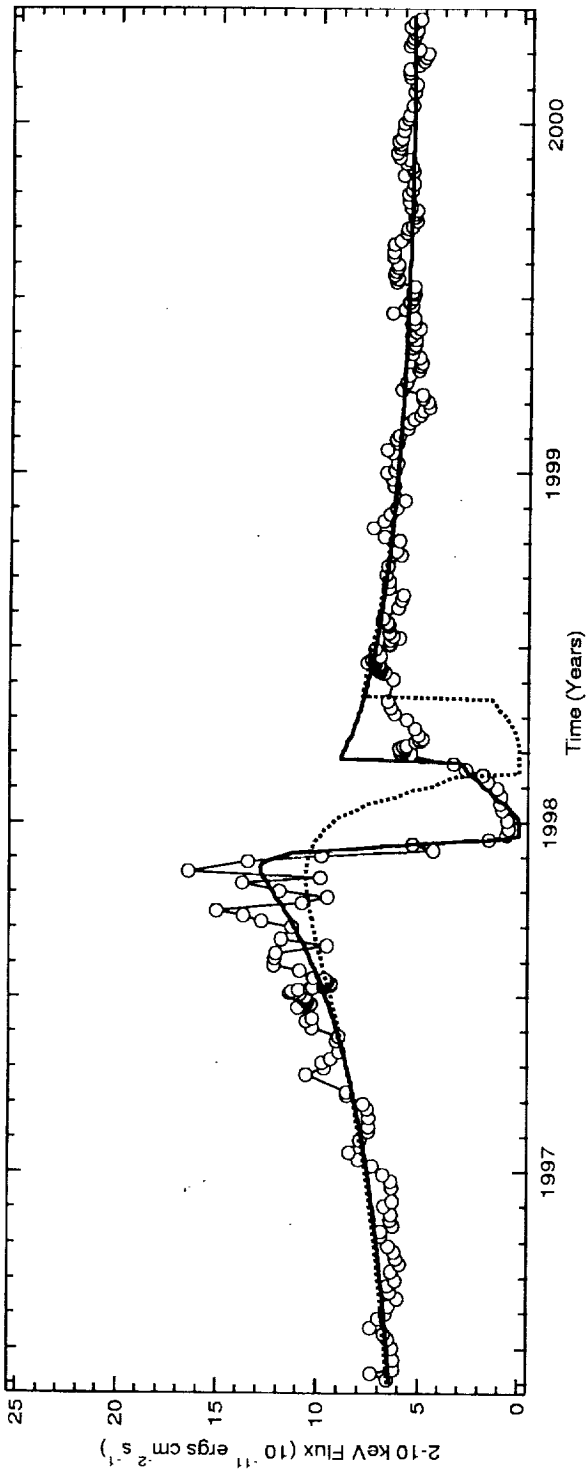
Fig. 3.— The *RXTE* lightcurve of η Carinae and the colliding wind model (see Table 1), including an interval of enhanced mass loss following periastron passage using the parameters in Table 1, along with an enhanced mass loss model based on the Damineli et al. (2000) parameters. The extra mass loss from the primary has the effect of suppressing the observed flux from the system for an extended period following periastron passage, and provides a better match to the duration of the X-ray eclipse.

Fig. 4.— The variation in N_H to the colliding wind shock. The “enhanced- \dot{M}_η ” model is shown by the thick line, and the “constant- \dot{M}_η ” model is shown by the thin line. The “enhanced- \dot{M}_η ” model provides an extended interval of extra absorption ($N_H > 10^{24} \text{ cm}^{-2}$) which completely hides the colliding wind shock.

Fig. 5.— The expected radial velocity curve of the primary based on the orbital elements derived in the present work (solid line) and on the Damineli et al. (2000) orbital elements (dotted line). The $v_{0.7}$ velocities from the STIS data reported by Davidson et al. (2000) are also shown.







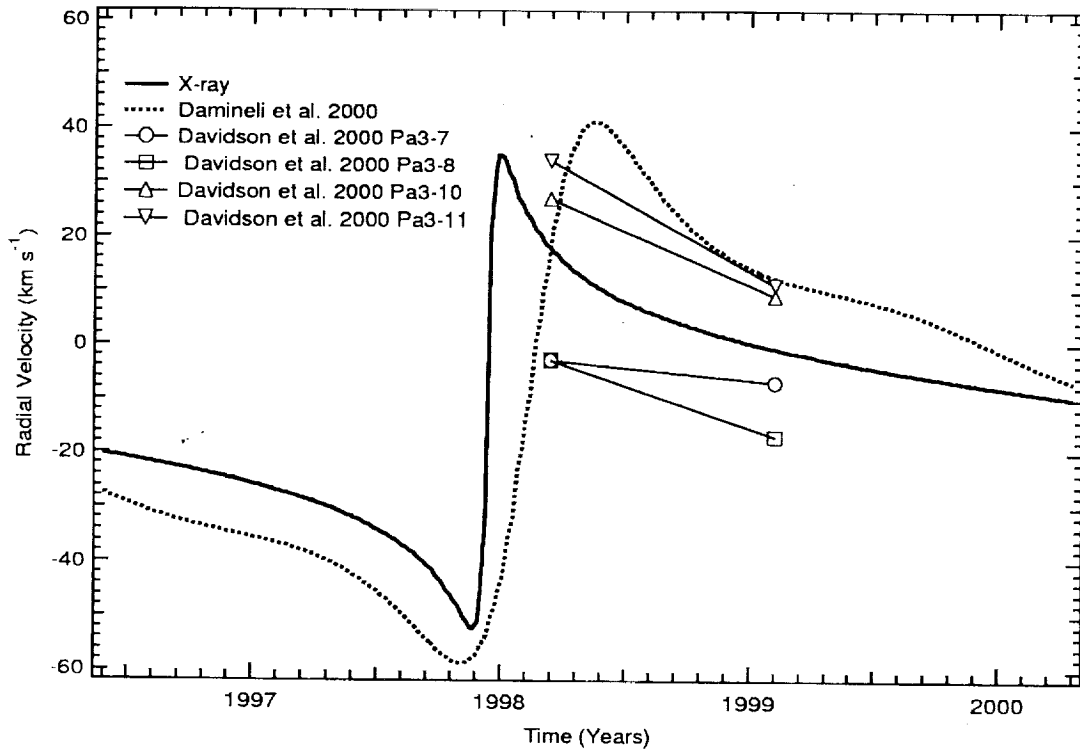
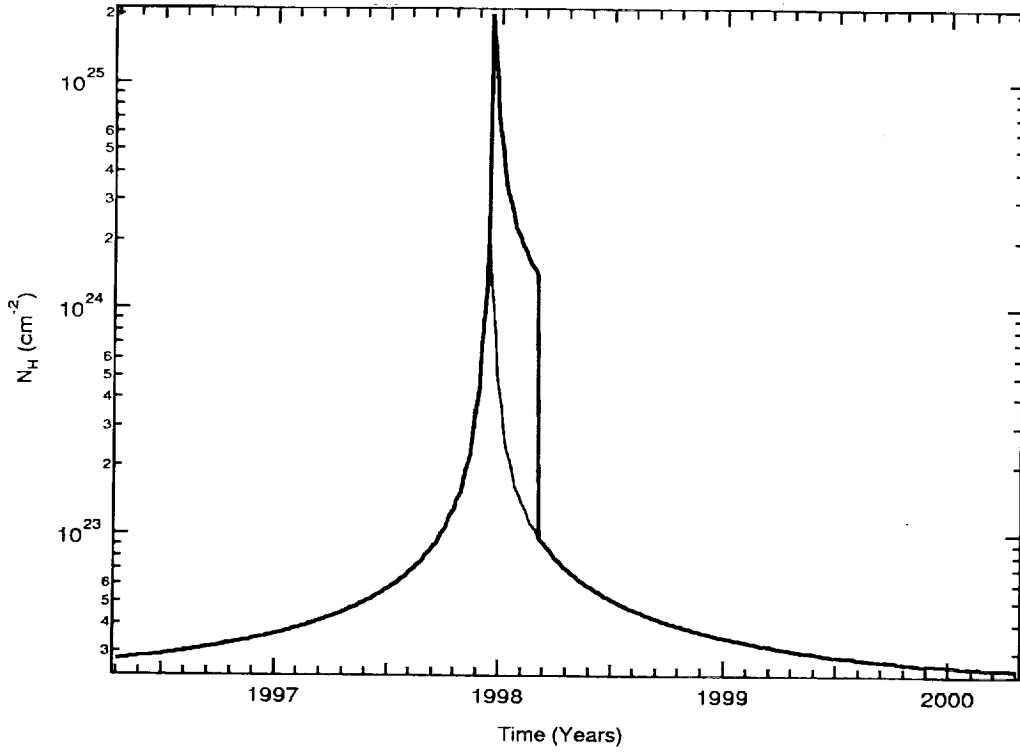


Table 1. Colliding Wind Model Parameters

Parameter	Present Work	Damineli et al. 2000 Value
T (periastron)	1997.95 ± 0.05	1998.13
e	0.90	0.75
P	5.52 years	5.53 ± 0.01
M_η	$80 M_\odot$	70
M_c	$30 M_\odot$	68
ω		275°
i		50°
γ		-12 km s^{-1}
\dot{M}_η		$10^{-4} M_\odot \text{ yr}^{-1}$
\dot{M}_c		$10^{-5} M_\odot \text{ yr}^{-1}$
$V_{\infty,\eta}$		500 km s^{-1}
$V_{\infty,c}$		2000.0 km s^{-1}